IOP Conf. Series: Materials Science and Engineering **400** (2018) 082019 doi:10.1088/1757-899X/400/8/082019

Computer fluid dynamics (CFD) study of new innovative backflow marine propeller

L C Stan[1], I Calimanescu[2] and V Popa[3]
[1,3]Maritime University of Constanța- România, Faculty of Naval Electromechanics, Department Electromechanics, Blvd. Mircea cel Bătrân, No 104, 900663, Constanța, România
2-Nuclear Power Plant Cernavoda, Romania

E-mail: liviustan14@yahoo.com

Abstract. There were many solutions to increase the marine propellers efficiency, like Propeller Boss Cap Fins, Tip Fins, Surface Piercing Propellers, Pre and Post-Swirl Devices, Ducted Propulsors etc.
All of them are supposing sometimes intricate devices involving high implementation costs and/or maintenance.
The present paper is proposing a new innovative Backflow Propeller where the core element is the backflow shield (or screen) which is inbuilt in the phase of fabrication stage of the propeller claiming zero mainenance costs.
As demonstrated via Ansys CFX the suction pressure on the blade back is increased 8 times which is easying the rotation of the propeller with the added benefit of the turning component of the backflow jet.
The downside of this innovative solution would be the increased thickness of the blade and the opposing component of the backflow jet, both affecting negativelly the eficiency.
What is missing here is the experimental validation. This is because any experimental research is to be conducted in dedicated laboratory with proper instrumentation. Therefore the Author is kindly inviting the researchers of interest to develop the experimental studies required and to come with the final figure of the efficiency improvment factor of the proposed solution.
Please bear in mind that the invention is protected by a Patent according to the International laws.

1. Introduction

One of the targets of any ship Owner is nowadays to decrease the operation costs. One solution is to use of so-called power saving devices like Propeller Boss Cap Fins, Tip Fins, Surface Piercing Propellers, Pre and Post-Swirl Devices, Ducted Propulsors etc.; these are stationary devices positioned near the propeller that improve the overall propulsion efficiency.

This paper introduces a novel approach, a Backflow Propeller. This power-saving device consists of a classical propeller to which was added a backflow screen with jet holes on the aft side as seen in the figure 1.

The device essentially reduces the rotational losses in the resulting propeller suction pressure on the blade back and increases the efficiency by creating a backflow jet.

The study of any blade pressure distribution arising from both loading and thickness effects has been undertaken so far and analytical methods were developed and put in place.

Before all, one has to look at some formulas regarding the pressures of fluid on the blade face/back.

The lifting surface theory is applicable to marine propellers suppose that the blades are lying on a helicoidal surface and is operating in a non-uniform flow of a fluid both incompressible and ideal. It is formulated by means of the acceleration potential method. [1]

The small perturbation approximation and the propeller blades are thin and operate without cavitation and flow separation are the basic assumptions of this approach.

The lifting surface S generates a pressure field given by distributed doublets with axis parallel to the local normal and with strength equal to the pressure jump across the surface.

Whether is introduced the acceleration potential function ψ which is a scalar function of position and defined as having its gradient equal to the acceleration vector, then the strength of the doublet distribution is proportional to the discontinuity of ψ between the values for the positive- and negative-oriented surfaces with respect to the direction of the normal $\vec{n}$, that is [2]:

$$\Delta\psi = \psi_+ - \psi_- = \frac{1}{\rho_f}\left(P_- - P_+\right) = \frac{1}{\rho_f}\Delta P \tag{1}$$

If one involves the linearized relation between the acceleration potential and the perturbation pressure, namely

$$\psi = -\frac{P}{P_f} \tag{2}$$

where P is local pressure and ρ_f is the fluid mass density. Thus, the pressure jump is defined as that between the pressure at the back (suction side) and the pressure at the face (pressure side) of the blade. The pressure P at any point (x, r, ϕ) in cylindrical coordinates at time t due to all pressure doublets distributed over dummy (loading) points (ξ, ρ, θ) will be given by:

$$P(x,r,\phi,t) = \frac{-1}{4\pi}\iint_S \Delta P(\xi,\rho,\theta,t)\frac{\partial}{\partial n}\frac{dS}{R'(x,r,\phi,t,\xi,\rho,\theta)} \tag{3}$$

where $\frac{\partial}{\partial n}$, is the normal derivative on the surface S at the loading point (ξ, ρ, θ) with fi the unit normal vector having positive axial component, and

$$R'(x,r,\phi,t,\xi,\rho,\theta) = \left[\left(x-\xi\right)^2 + r^2 + \rho^2 - 2r\rho\cos(\theta-\phi)\right]^{1/2} \tag{4}$$

is the Descartes distance between the given control point (x, r, ϕ) and the loading point (ξ, ρ, θ).

The total pressure distribution on each blade face should be the superposition of the pressure P_T due to the thickness effect, which produces no lift, on the pressures arising from the effects of "nonplanar" thickness, camber and angle of attack of the blade and of spatial nonuniformity of the inflow field. The last four components contribute to the lift because each produces a pressure difference ΔP between the back and front faces of the blade surface. On the suction side (back face) the pressure due to the loading contributors is $\Delta P/2$; on the pressure side (front face) the pressure is $-\Delta P/2$.

Since the blade is considered to be rigid, the nonlifting thickness effect will be present only in the steady state. In this case (q = 0) the blade pressure distribution is made up as follows:

(a) On the pressure side

$$P_P^{(0)} = -\left(\frac{\Delta P}{2}\right)_w^{(0)} - \left(\frac{\Delta P}{2}\right)_c - \left(\frac{\Delta P}{2}\right)_f - \left(\frac{\Delta P}{2}\right)_{npt} + P_r \tag{5}$$

(b) On the suction side

$$P_s^{(0)} = \left(\frac{\Delta P}{2}\right)_w^{(0)} + \left(\frac{\Delta P}{2}\right)_c + \left(\frac{\Delta P}{2}\right)_f + \left(\frac{\Delta P}{2}\right)_{npt} + p_r \quad (6)$$

where the subscripts, w, c, f, and npt refer to wake, camber, flow angle, and "nonplanar"' thickness, respectively.

The formulas (5) and (6) above are demonstrating the common knowledge that the pressures on the blade face and blade back are different, namely the face is pushing the fluid whereas the back is sucking the fluid.

The blade face is developing the useful pressure for the ship motion but the suction pressure on the blade back is consuming the engine power with no avail.

Whether one can figure out a certain device to diminish the suction pressure then the propeller efficiency is by all means improved.

Such a device is described in the followings.

2. Materials and methods

2.1 Invention description

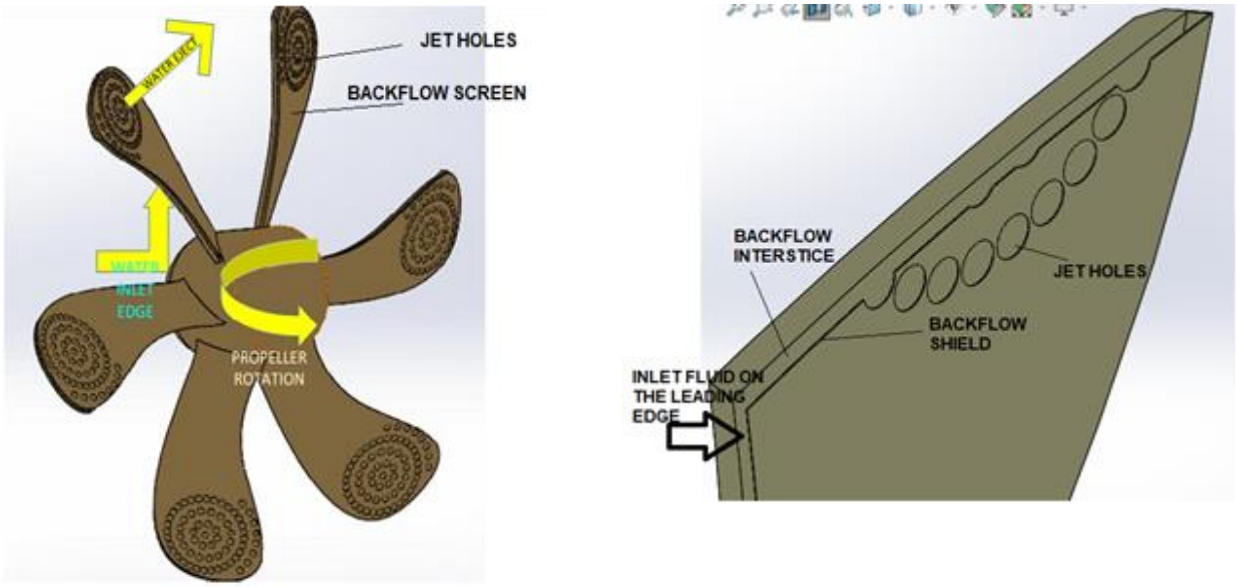

Figure 1. The backflow propeller.

Since was already demonstrated that the suction pressure exerted on the aft side of the propeller blade is the main contributor in decreasing the propeller efficiency, the new proposed backflow propeller is simply a classical propeller to which was added a backflow screen (or shield) with jet holes on the aft side as seen in the figure 1 [3]. The backflow screen (or shield) is doubling the aft face of the blade leaving in between a backflow interstice. The backflow shield is closed in all directions leaving just one opening on the leading edge for the incoming fluid pushed here by the propeller rotation. In very plain words, the backflow interstice/screen (shield) is collecting the fluid from the leading-edge due to the rotation motion, and is directing it toward the jet holes in order to obtain the backflow jet.

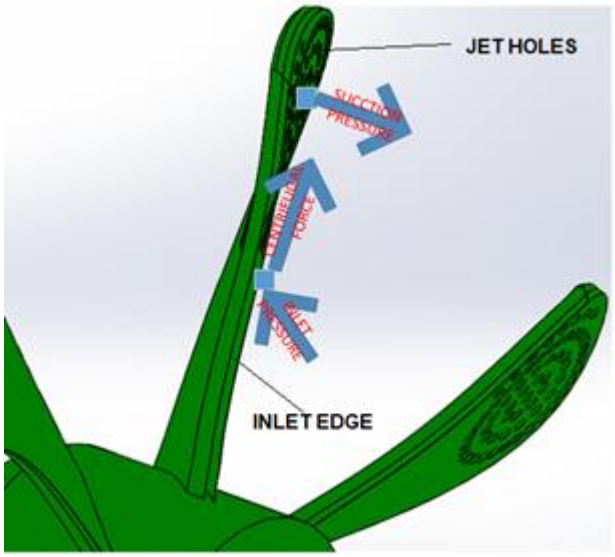

Figure 2. Forces acting on a fluid particle.

The inlet edge of the backflow screen is placed as to allow a small quantity of fluid to enter inside the space between the aft side of the propeller and the backflow screen (backflow interstice). Once there, the fluid particle is subjected to a series of forces which will push the particle to form a jet inside the jet holes.

On the inlet edge of the backflow screen the rotation motion of the propeller if forcing the fluid particle to develop a certain pressure. There the kinetic pressure is translated into a static pressure.

The fluid particle is then forced to follow the blade rotation hence a centrifugal force will be developed here to push further the particle toward the jet holes (figure 2).

Once arrived in the jet holes region the suction pressure naturally existing there will suck the particle to form a backflow jet. This fluid jet is diverting the whirlpools mainly responsible for the suction pressure and the suction pressure itself is fed decreasing its intensity and increasing the propeller efficiency.

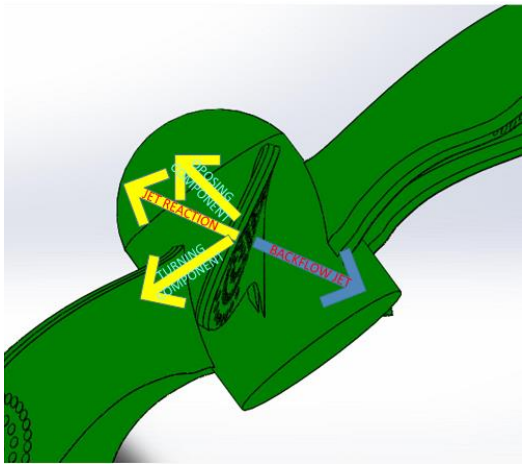

Figure 3. Jet reaction components.

The backflow jet will develop a jet reaction force as seen in the figure 3, with two components: the Opposing Component which will tend to oppose to the ship motion and the Turning Component which will help the propeller to rotate.

In theory, the jet holes can be placed wherever the designer may deem appropriate on the backflow shield. The placement of the jet holes on the tip of the blade is following two rationales: firstly, the tip

of the blade is fostering the biggest suction pressure as we'll see in the followings, and, secondly, the bigger is the force arm between the propeller axis and the jet holes' region, the bigger the turning component moment will be [4].

2.2. The CAD Models of the classical and innovative propellers

In this paper, we will develop two series of numerical experiments: firstly, the classical propeller Computer Fluid Dynamics analysis as opposed to the new innovative backflow propeller. In order to have meaningful results, the two propellers have the same dimensions and geometry and the Finite Volumes Elements Analysis (FVEA) involving Ansys 16 CFX, will have exactly the same parameters.

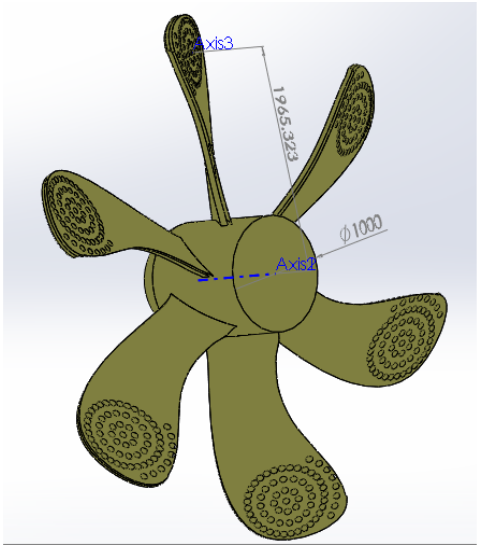

Figure 4. The innovative backflow propeller.

In the figure 4 is to be seen the innovative backflow propeller with six blades and the hub diameter of 1000 mm. The central jet hole axis is placed at 1965 mm from the propeller axis. The propeller was designed using SolidWorks 2016.

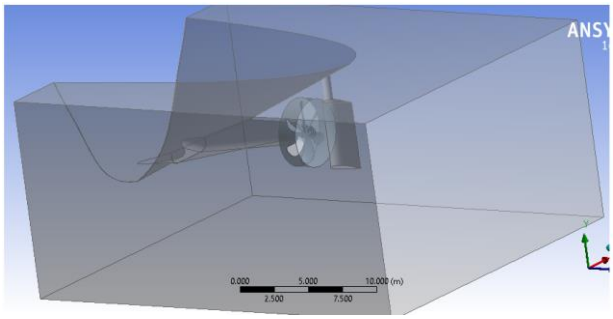

Figure 5. The fluid domain of the simulation

The fluid domain as exported inside Ansys 16 CFX is comprising the aft of the ship together with the rudder in order to have the most realistic results possible (see figure 5).

2.3. The FVEA Model

The FVEA model was developed inside Ansys 16 CFX by importing the 3D model inside the Design Modeller.

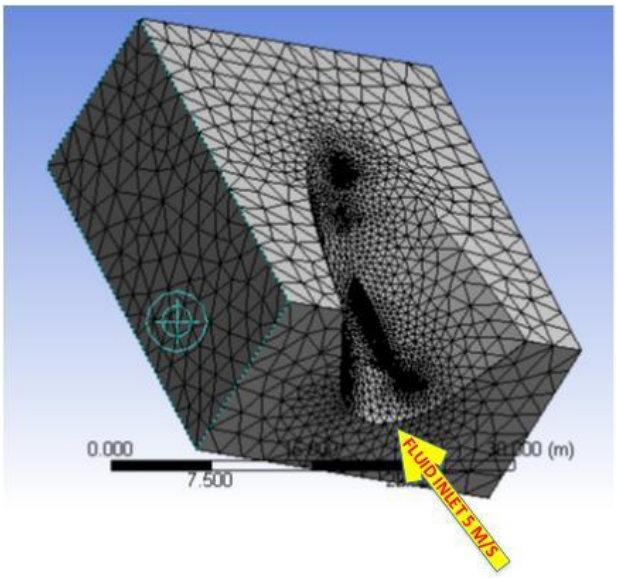

Figure 6. The Finite volume mesh of the fluid domain.

The meshing is made out of finite volume elements. The meshing comprises 270769 finite volume elements with 48852 nodes.

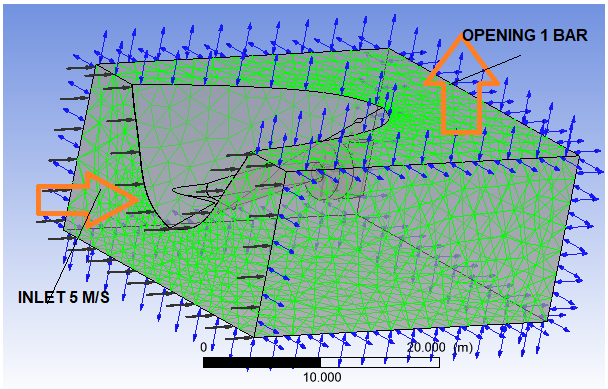

Figure 7. The boundary conditions.

The boundary conditions imposed to the model are the Inlet fluid velocity 5 m /s to mimic the ship motion and the Opening boundary with relative pressure 1 bar as seen in figure 7.

The fluid is water with the well-known properties.

The turbulence will be modelled with the classical k-omega model and the fluid domain of the propeller is rotating with 120 RPM. The interface between the propeller and the fluid domain is General Connection with the Frame change model Frozen Rotor.

3. Results and discussion

3.1 The Streamlines

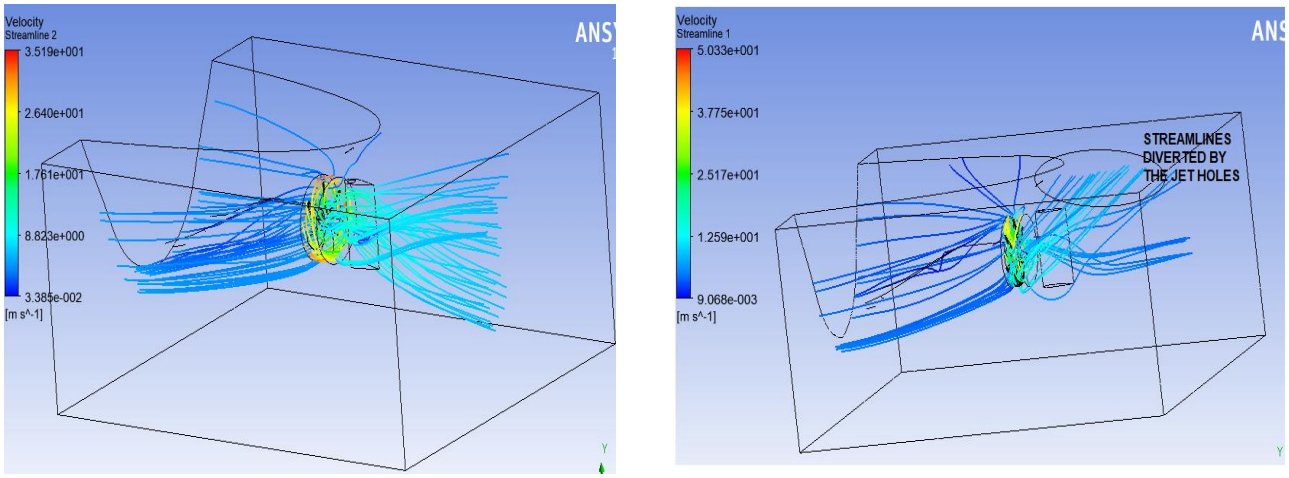

a - Normal propeller b - Backflow propeller

Figure 8. Streamlines for the two models.

By analysing the streamlines for the two models it's obvious that the Jet Holes are diverting the streamlines in an oblique direction as seen in figure 8. The first conclusion is that the backflow shield is working since the stream lines are affected by the presence of jet holes on the backflow shield.

3.2 The velocities fields on a vertical plane

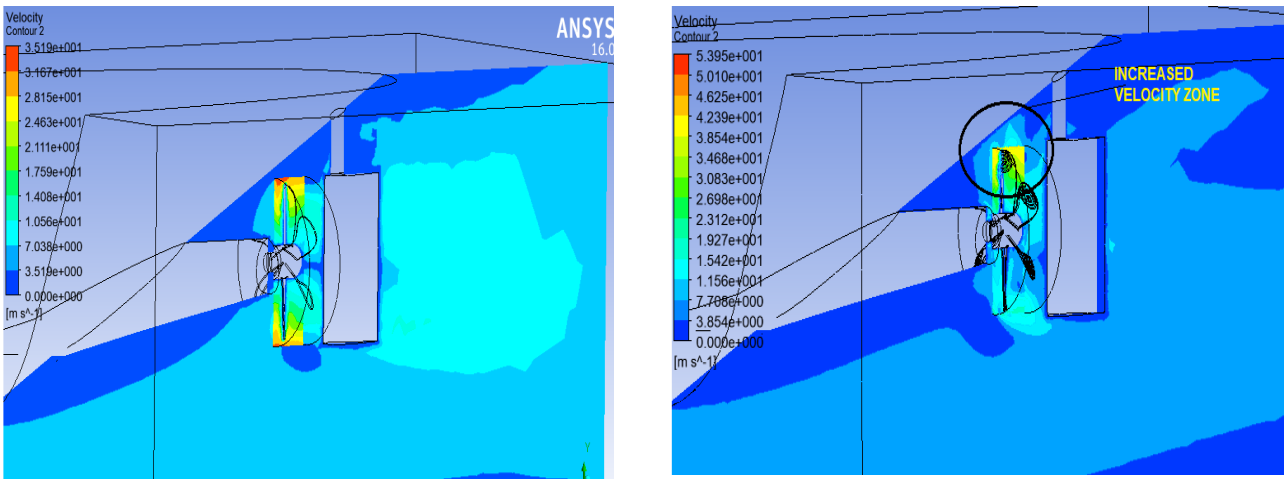

a - Normal propeller b - Backflow propeller

Figure 9. Velocities fields in vertical plane for the two models.

The velocities calculated for the normal propeller are reaching a maximum of 35.18 m/s at the tip of the blades whereas for the backflow propeller the maximum velocity is 53.95 m/s in the jet holes region. The shape of the velocity field for the backflow propeller is skewed due to the backflow jets.

3.3 The pressures fields on a vertical plane

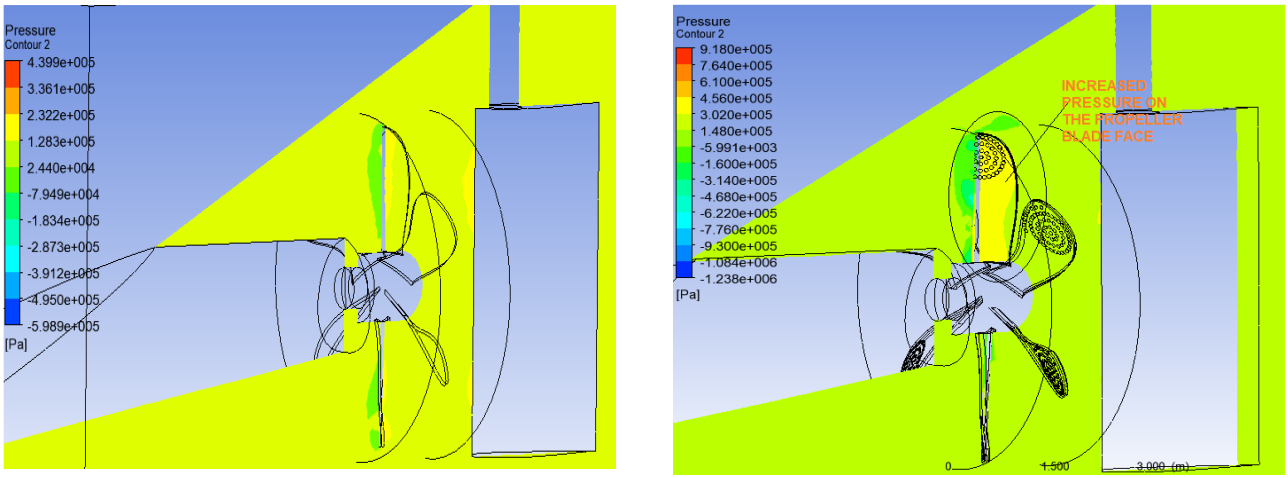

a - Normal propeller b - Backflow propeller

Figure 10. Pressure fields in vertical plane for the two models.

The peak pressures for the backflow propeller are almost double as compared to the normal propeller ones (9.1 10^5 Pa /4.3 10^5 Pa). Moreover, on the blade face region a bigger pressure is calculated, as seen in figure 10.

3.4 The velocities fields on a horizontal plane going through the jet holes

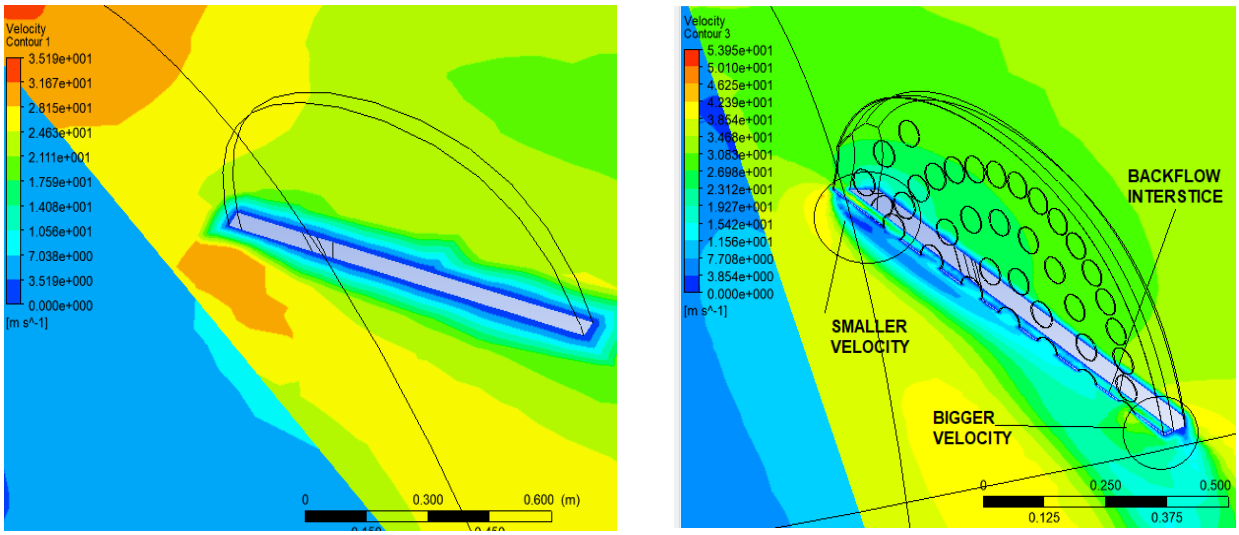

a - Normal propeller b - Backflow propeller

Figure 11. Velocity fields in a horizontal plane going through the jet holes for the two models.

The normal propeller has no backflow shield (screen) and jet holes.

By analysing the figure 11 above it is obvious that the fluid inside the backflow interstice is migrating through the jet holes to form the backflow jet. The biggest velocity (31 m/s) is computed for the holes near the trailing edge whereas the pressure is smaller, whereas the smallest velocity is computed for the holes near the leading edge of the blade (6 m/s) where the pressure is the biggest.

3.5 The pressure fields on a horizontal plane going through the jet holes

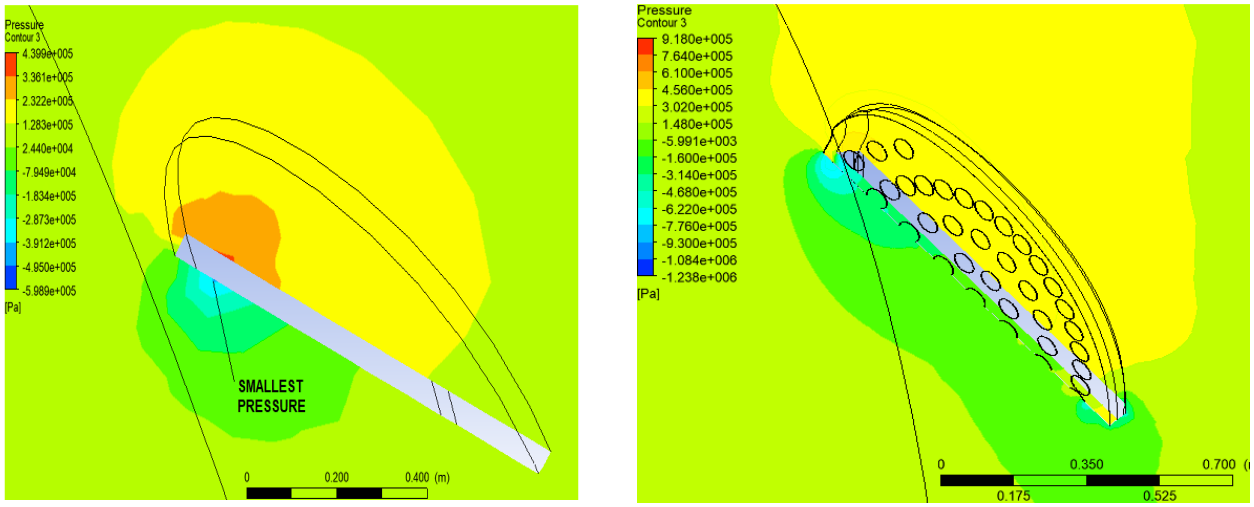

a - Normal propeller b - Backflow propeller

Figure 12. Pressure fields in a horizontal plane going through the jet holes for the two models.

The shape of the pressure fields for the backflow propeller as compared to the normal propeller is obviously altered (figure 12). The suction pressure in the jet holes region is diminished with a value to be seen in the following figures.

3.6 The pressure fields on the blade faces

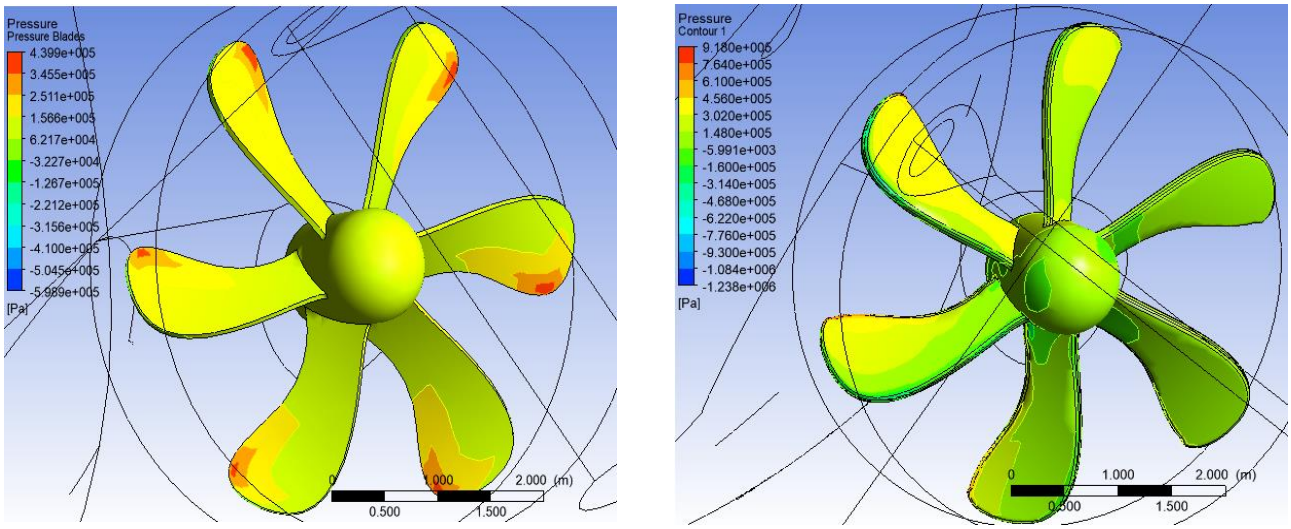

a - Normal propeller b - Backflow propeller

Figure 13. Pressure fields on the blade faces.

The shapes of the pressure distribution fields are similar for the two cases with the difference that the peak pressure values for the backflow propeller is higher since the leading edge of the blade was geometrically altered by the backflow shield. By calculating the average pressure for the blade faces, one can see that for the normal propeller it is 141453 Pa whereas for the new type it is 137719 Pa, almost equal.

3.7 The pressure fields on the blade back

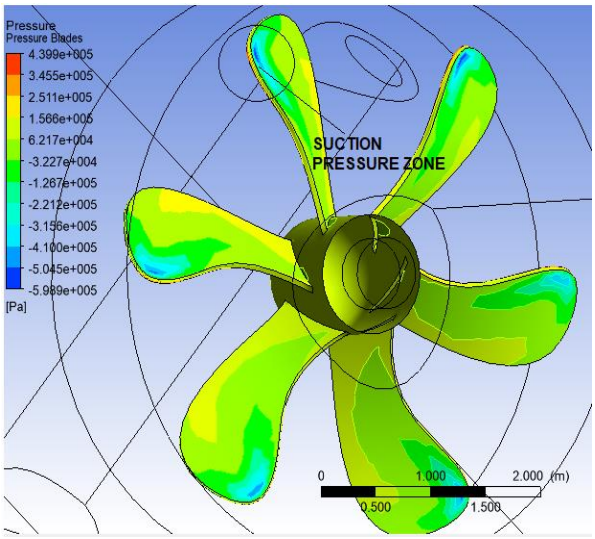

a - Normal propeller

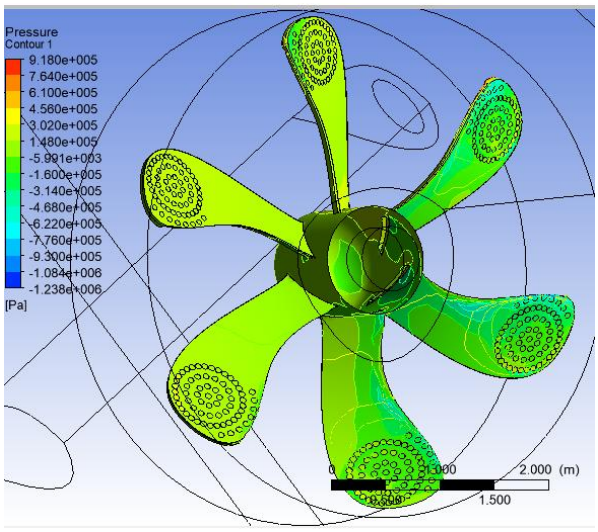

b - Backflow propeller

Figure 14. Pressure fields on the blade back.

The shapes of the pressure distribution fields are different for the two cases meaning that the suction pressures for the tip of the blade are now diminished for the innovative propeller. By calculating the average pressure for the blade faces, one can see that for the normal propeller it is 7288.2 Pa whereas for the new type it is 59483.9 Pa, almost 8 times bigger. This is underlining the effectiveness of the new innovative backflow propeller to which the suction pressure is dramatically increased so that the efficiency of the propeller will increase.

4. Conclusions

There were many solutions to increase the marine propellers efficiency, like Propeller Boss Cap Fins, Tip Fins, Surface Piercing Propellers, Pre and Post-Swirl Devices, Ducted Propulsors etc.

All of them are supposing sometimes intricate devices involving high implementation costs and/or maintenance.

The present paper is proposing a new innovative backflow propeller where the core element is the backflow shield (or screen) which is inbuilt in the phase of fabrication stage of the propeller claiming zero mainenance costs.

As demonstrated via Ansys CFX the suction pressure on the blade back is increased 8 times which is easying the rotation of the propeller with the added benefit of the turning component of the backflow jet.

The downside of this innovative solution would be the increased thickness of the blade and the opposing component of the backflow jet, both affecting negativelly the eficiency.

What is missing here is the experimental validation. This is because any experimental research is to be conducted in dedicated laboratory with proper instrumentation. Therefore the Author is kindly inviting the researchers of interest to develop the experimental studies required and to come with the final figure of the efficiency improvment factor of the proposed solution.

Please bear in mind that the invention is protected by a Patent according to the International laws.

5. References

[1] Stan LC and Calimanescu I 2016 *Computer fluid dynamics (CFD) study of a plate heat exchanger working with nanofluids, Proceedings of SPIE 0277-786X, V, Volume 10010, Proceedings of SPIE - Advanced Topics in Optoelectronics, Microelectronics, and Nanotechnologies VIII, Section Modeling, design, and simulation*, pp 11-21, DOI: 10.1117/12.2257302, Constanta

[2] Tsakonas S and Jacobs W R 1979 Propeller Blade Pressure Distribution Loading and Thickness Effects, *Journal of Ship Research* **23**(2) 89-107

[3] Martinas G, Cupsa S, Stan L C and Arsenie A 2015 Cold flow simulation of an internal combustion engine with vertical valves using layering approach *IOP Conference Series: Materials Science and Engineering* **95** no 012043

[4] Stan LC and Buzbuchi N 2010 Operation Factors Influence on the Dynamics Behavior of Marine Propulsion Systems, *Proceedings of the Advanced Manufacturing Engineering, Quality and Production Systems, 2nd International Conference on Manufacturing Engineering, Quality and Production Systems (MEQAPS'10*), pp 29-33, ISSN: 1792-4693, ISBN: 978-960-474-220-2, Constanta available at http://www.wseas.us/e-library/conferences/2010/Constantza/MEQAPS/MEQAPS-00.pdf

[5] ANSYS 16 - Users'manual 2013

[6] Calimanescu I and Stan LC 2012 Elice de propulsie acvatică cu pale cu ajutaje laterale şi dorsale, cu rezistenţă hidrodinamică diminuată, *Patent no. A 2012 00667 /20.09.2012*, published in the Official Industrial Property Bulletin - Inventions Section No. 3, Bucharest